Binding Energies in Atomic Negative Ions: II

H. Hotop[a] and W. C. Lineberger

Department of Chemistry and Joint Institute for Laboratory Astrophysics, University of Colorado and National Bureau of Standards, Boulder, Colorado 80309

This article updates a ten-year-old review of this subject [J. Chem. Phys. Ref. Data **4**, 539 (1975)]. A survey of the electron affinity determinations for the elements up to $Z = 85$ is presented, and based upon these data, a set of recommended electron affinities is established. Recent calculations of atomic electron affinities and the major semiempirical methods are discussed and compared with experiment. The experimental methods which yield electron binding energy data are described and intercompared. Fine structure splittings of these ions and excited state term energies are given.

Key words: *ab initio* calculations; atomic negative ions; binding energy; electron affinity; excited states; experimental methods; fine structure splitting; recommended values; semiempirical calculations.

Contents

List of Tables

List of Figures

[a] On leave from Fachbereich Physik, Universität Kaiserslautern, 6750 Kaiserslautern, Federal Republic of Germany.

1. Introduction

Ten years have passed since we attempted[1] to review critically and compile the knowledge of binding energies in atomic negative ions. The development of tunable dye lasers and intense cw ion lasers in the late 1960's had opened new horizons for negative ion spectroscopy, and by 1975, the electron affinities of 19 atoms had been determined by laser photodetachment. Since the publication of that review, this number has increased to 40, and the effective resolution both in threshold experiments and in electron spectrometric studies has been improved substantially. The electron affinities of the atoms O and S are now known to within 0.01 cm^{-1} (relative uncertainty 5×10^{-7})!

This review differs from the 1975 article to a large extent. Here, we concentrate on new developments in negative ion spectroscopy and try to inform the readers (especially those who are nonexperts) about the basic aspects of laser photodetachment experiments, the principal limitations to the resolution, and the present status of threshold studies and photoelectron spectrometry of negative ions. We hope that this information will be useful in interpreting uncertainties given in the data tables and provide a feel for possible future developments and improvements.

Since 1975, several review articles[2–8] and a monograph[9] have dealt with negative ion spectroscopy, and some of them contain updated information on atomic electron affinities. Drzaic, Marks, and Brauman[8] provide the most complete source of accurate molecular electron affinities. In this paper, we emphasize those aspects relevant for reliable and accurate determination of atomic negative ion states and their binding energies. We summarize the present knowledge by providing tables of the atomic electron affinities and of the fine-structure splitting in several ions.

2. Calculation of Atomic Electron Affinities

The electron affinity EA of an atom A is the difference between the total energies (E_{tot}) of the ground states of A and its negative ion A^-:

$$EA(A) = E_{tot}(A) - E_{tot}(A^-). \quad (1)$$

By ground state, one implies the lowest energy hyperfine-structure level of A and A^-, respectively. The quantity EA (A) is positive if the stable negative ion A^- exists. The total energy can be written as

$$E_{tot} = E_{HF} + E_C + E_{SO} + \delta. \quad (2)$$

E_{HF} corresponds to the (restricted) Hartree–Fock energy, E_C is the nonrelativistic correlation energy describing the deviation of the many electron system from the Hartree–Fock (HF) self-consistent field model, E_{SO} is the spin-orbit energy for states with nonzero orbital angular momentum and spin, and δ comprises correction terms including hyperfine structure, mass polarization, and radiation effects (Lamb shift).

In the 1975 review,[1] we presented a rather complete survey on the status of semiempirical and *ab initio* calculations of atomic electron affinities. Since then, some further important contributions have been made. They concern the stability of negative ions (see, for example, the work by Lieb[10] and references therein), a rather accurate computation of EA (Li) = 0.609(7) eV,[11] and the calculation of the binding energies in several long-lived excited states of ions,[12–19] such as $He^-(1s2s2p\ ^4P^o)$,[14,18,19] $He^-(2p^3\ ^4S^o)$,[18] and $Li^-(^5P^e, ^5S^o)$.[15,16] A comprehensive overview of the status of atomic electron affinity calculations was given by Bunge and Bunge[12] in 1978.

For H^-, *ab initio* theory is clearly ahead of experiment with regard to the determination of EA (H).[20,21] In order to test the theoretical EA (H),[1] known to within 0.02 cm^{-1}, a coaxial laser-ion beam experiment would have to determine the p-wave photodetachment threshold in the infrared (now in principle accessible with a single mode F_2^+ color center laser) to within 0.01 cm^{-1}. An estimate of the cross section 0.01 cm^{-1} (300 MHz) above the threshold for the $H^-(F=1/2)\rightarrow H(F=0)$ transition, based upon Wigner's threshold law[22] and absolute cross sections of Broad and Reinhardt,[23] yields a value around 10^{-24} cm^2, which is not very inviting!

Ab initio calculations for negative ions with three and four electrons have now been perfected to such a degree that the results are competitive or even more precise than the available experimental results. For high-lying metastable excited states, the predictive character of such calculations[14–18] is of great value to the experimentalist, who is trying to produce and detect such states,[24–31] e.g., by sequential charge exchange of positive ions.[30,31]

For larger systems, the situation has not changed substantially since 1975. The uncertainty of *ab initio* predictions is in the range 0.1–0.3 eV.[1,12,32,33] For the transition metal atoms, semiempirical methods (e.g., horizontal analysis)[1,34] has been used and found useful.[1] Two recent papers have dealt with the electron affinity of atoms in the lanthanide series. Angelov[35] used empirical formulas to calculate EA's from the first ionization potential and radial integrals $\langle 1/r\rangle$ for the neutral lanthanides. The elements La, Ce, Pr, Nd, Pm, Sm, and Gd are predicted to form stable negative ions with binding energies between 0.2 and 0.8 eV. Cole and Perdew[33] predict stability for the negative ions of Ce, Pr, Nd, and Gd. Bratsch[36] used spectroscopic information on energy variations associated with changes in the $4f$ orbital population of the lanthanides to predict their EA's with an estimated uncertainty of $\pm$ 0.3 eV. He found that all EA's are in the range $-$ 0.3 to 0.5 eV, with stable negative ions formed by La, Ce, Sm, Gd, Tb, Tm, and Lu. For more details and the

individual numbers, the reader is referred to the original paper. Bratsch and Lagowski[37] have also made similar estimates for the actinides. Unfortunately, there exist no data which test the accuracy of these estimates for the lanthanides and the actinides.

3. Experimental Aspects of Negative Ion Spectroscopy

3.1. Introductory Remarks

The principle of the laser photodetachment method is to have a well-specified sample of negative ions A^- interacting with a beam of (tunable) monochromatic light in a region free of static external fields and with low density of background gas. One normally measures the detachment products (neutral atoms and/or electrons) either by utilizing a tunable light source to detect onsets (thresholds) due to allowed bound-free transitions [laser photodetachment threshold (LPT) studies] or by energy analyzing the detached electrons [laser photodetached electron spectrometry (LPES)]. The basic requirements therefore are: (i) suitable sources for the production of the negative ions A^-, (ii) sufficiently intense lasers (preferably cw lasers) with narrow bandwidth, (iii) ultrahigh vacuum in the interaction region, and (iv) sensitive product detection and high resolution electron energy analysis.

With either experimental arrangement, one still must make a choice for the geometry of the experiment. Until 1975, crossed ion and laser beams were used both in threshold photodetachment[1,38–44] and in photoelectron spectrometric studies.[1,42–46] A simple consideration of the kinematics of photon absorption and electron emission shows (see below), however, that potentially the highest resolution is obtained with coaxial alignment of the ion and photon beams[47–51] (LPT) and electron detection parallel or antiparallel to the ion beam[52–53] (LPES). The coaxial choice for ion and photon beam has been exploited by many groups carrying out laser spectroscopy on fast positive and negative ion beams, whereas in LPES, this approach has not been utilized. At present other factors provide the limiting resolution in LPES. Before discussing selected experiments in Secs. 4 and 5 we mention briefly the current status of the subjects (i)–(iv) and comment on the basic problems which limit the resolution in LPT and LPES experiments.

3.2. Sources for Atomic Negative Ions

Negative ion source technology is well developed[25–29] in connection with their use in tandem accelerators. Penning-type sources[25] have been used by Feldmann *et al.*[54–60] in photodetachment studies, and Heinicke *et al.*[25,26] showed that this ion source is capable of producing intense beams of essentially all stable negative ions in the main groups of the periodic table. Sputter ion sources[27–29] are especially suited to produce ion beams of refractory metals, and a scaled-down version[61] of the source described by Middleton[28] was used by Feigerle *et al.*[62–64] in recent LPES measurements of the electron affinity (EA) of more than a dozen transition metal atoms. In studies of atomic negative ions, the presence of excited states (e.g., fine-structure excited states) in the beam normally does not produce major problems in the interpretation of data (see, for example, Feigerle *et al.*[62]). Therefore the use of "hot" ion sources such as the sputter source[61] is not a significant disadvantage. A matter of concern may lie in the kinetic spread often associated with low-pressure ion sources, but in LPES experiments with perpendicular electron detection even an energy spread around 10 eV at about 1-keV ion energy is not the resolution-limiting factor.

For special cases, e.g., for the information on metastable states such as $He^-(^4P^e)$[42,65] or $Be^-(^4P^e)$,[31] it can be advantageous to use two-stage charge exchange of a positive ion beam in neutral gases such as Cs vapor.[30,31,42,65] To summarize, one can say that present day ion source technology is capable of producing sufficiently intense beams of all stable and many metastable atomic negative ions such as to allow photodetachment measurements of their binding energies.

3.3. Laser Properties, Signal Considerations

Until 1977, LPT studies were carried out with pulsed lasers[38–41,57,58,66] (mainly flashlamp-pumped dye lasers[38–41]) with a typical resolution of 4 cm^{-1}. The low duty cycle of these systems was in part compensated by the background discrimination through time-gated product detection. Since then, several groups[51,65,67–73] have started to use cw dye lasers with good success. Typical output powers range from 0.1–1 W; with state-of-the-art cw ring dye lasers, commercially available since about 1980, this power is contained in a single longitudinal mode which can be continuously scanned over 30 GHz (1 cm^{-1}) or even, with computer control, over a region of about 1000 GHz ($\approx$30 cm^{-1}).

It is illustrative to give the signal-to-background ratio for typical conditions: the probability p_γ for photodetachment is given by

$$p_\gamma = I_\gamma \sigma_\gamma L / v E_\gamma, \tag{3}$$

where I_γ = laser intensity, E_γ = photon energy, v = ion velocity, σ_γ = photodetachment cross section, and L = length of interaction region. With $I_\gamma = 10$ W/cm^2, $E_\gamma = 3\times10^{-19}$ J($\approx$2 eV), $\sigma_\gamma = 10^{-18}$ cm^2, $L_\gamma = 0.3$ cm (crossed beams), $v = 10^7$ cm/s, one estimates $p_\gamma \approx 10^{-6}$. The probability p_d for detachment in collisions of negative ions with the background gas (density n) is given by

$$p_d = \sigma_d n L_d. \tag{4}$$

With $\sigma_d \approx 10^{-15}$ cm^2, $n = 3\times10^7$/cm^3($p \approx 10^{-9}$ Torr), $L_d \approx 3$ cm, one has $P_d \approx 10^{-7}$. With these assumptions, a signal-to-background ratio of 10 is obtained. This can be improved by using an "intracavity" configuration (interaction region located in the laser cavity) with a resultant increase in I_γ by factors of 10–100. In addition, the favorable coaxial choice with essentially equal L_γ and L_d improves the signal to noise by another factor of 10 and increases the photodetachment signal by about a factor of 100 ($L_\gamma \approx 30$ cm). As a result, photodetachment processes with cross sections in the (10^{-21}–10^{-22}) cm^2 range can be measured with signal-to-background ratios around 1, if a coaxial, intracavity cw laser arrangement is used.

The resolution in threshold photodetachment studies is limited by kinematic broadening (see below). The frequency jitter of commerical stabilized cw ring dye lasers is $\lesssim 1$ MHz with long-term drifts typically below 100 MHz/h. Wave meters, e.g., traveling Michelson-type wave meters[74] using polarization-stabilized HeNe lasers as a reference,[75] present reliable instruments for an easy determination of the wavelength of the tunable laser to within $\pm$ 100 MHz, once they have been calibrated against an accurately known absolute standard. This level of accuracy corresponds to an *EA* determination to better than 1 μeV.

For the laser photodetachment electron spectrometry experiments, intense cw Ar-ion lasers have been utilized in an intracavity configuration, in which the ion beam interacts with the focused laser beam within the laser cavity. In this way, laser powers of typically 100 W are available for photodetachment. The frequency width of the multimode-ion lasers is around 10 GHz (4×10^{-5} eV) and is negligible in current LPES.

3.4. Kinematic Constraints on Resolution in Photodetachment Studies

As in any other optical absorption and electron spectrometric experiment, there are kinematic limits to the resolution which can be obtained in LPT and LPES experiments. Here, we confine the discussion to devices using crossed or coaxial ion and laser beams.

a. Limits to the Optical Resolution (Doppler Effect, Transit Time)

If an ion beam with velocity v interacts with a laser beam (frequency ν_L, propagation direction along unit vector $\hat{e}_L$) the ions "see" an effective frequency ν_{eff} given by

$$\nu_{eff} = \nu_L \frac{1-\hat{e}_L\cdot v/c}{[1-(v/c)^2]^{1/2}}. \tag{5}$$

As a result of the finite divergence $\Delta\theta$ of the ion and the laser beams (the divergence of the latter can be neglected in many cases), the optical transition acquires a bandwidth $\Delta\nu_{eff}(\Delta\theta)$.

For nonrelativistic beams crossed at right angles [$\theta = \sphericalangle(\hat{e}_L, v) = 90°$], one obtains

$$\Delta\nu_{eff}(\Delta\theta;90°) \approx \nu_L\cdot(v/c)\Delta\theta = (v/\lambda_L)\Delta\theta, \tag{6}$$

where λ_L is the vacuum wavelength of the laser. With numbers typical for crossed beam experiments ($v = 10^5$ m/s, $\lambda_L = 5\times10^{-7}$ m, $\Delta\theta = 0.02$ rad) one obtains $\Delta\nu_{eff}(\Delta\theta;90°) = 4$ GHz, indicating a severe limitation when using single mode lasers. Note, however, that an uncertainty of that order (16 μeV) is negligible for most practical purposes.

For coaxial beams, the absorption bandwidth due to beam divergence amounts to

$$\Delta\nu_{eff}(\Delta\theta;0°,180°) = \nu_L(v/c)\left[1-\cos\frac{\Delta\theta}{2}\right] \cong (v/\lambda_L)(\Delta\theta^2/8). \tag{7}$$

With v, λ_L, $\Delta\theta$ as above, one obtains $\Delta\nu_{eff} = 10$ MHz, demonstrating clearly the need to use coaxial beams for ultrahigh resolution work. Since the Doppler shift is greatest for coaxial beams, one has to consider the broadening $\Delta\nu_{eff}(\Delta v)$ due to the velocity spread Δv in the ion beam (which is negligible for crossed beams)

$$\Delta\nu_{eff}(\Delta v;0°,180°) = \Delta v/\lambda_L = \Delta W/(\lambda_L\sqrt{2MW}). \tag{8}$$

Here, W = ion kinetic energy, ΔW = ion beam energy spread, and M = ion mass. As an example, for a 4-keV $^{16}O^-$ beam with a spread $\Delta W = 1$ eV, one obtains at $\lambda_L = 5\times10^{-7}$ m a $\Delta\nu_{eff} = 55$ MHz. This frequency spread can be decreased, at a given ΔW, by choosing a higher kinetic energy.

We briefly mention the fundamental limitation due to the finite interaction time T of the ions with the laser beam. In both crossed and coaxial beams, the associated frequency width,

$$\delta\nu \approx (1/T) = (L/v), \tag{9}$$

is normally smaller than the limits set by beam divergence in crossed beams and by divergence and velocity spread in coaxial beams.

b. Limits to the Energy Resolution in Electron Spectrometry

In most of the photodetachment electron spectrometry studies carried out so far,[42–46,62–64] the resolution was limited by the electron spectrometer itself to values $\Delta E_s \approx 50$ meV. More recently, Breyer *et al.*[76,77] have achieved an overall resolution of about 5 meV with $\Delta E_s \approx 3$–4 meV attributable to the resolution of their hemispherical analyzer. Similar values were subsequently realized by Feigerle *et al.*[78] and appear to be the state of the art in current electron spectroscopy.[79]

The basic energy balance equation for photoelectron detection of an angle ϕ relative to the ion velocity in the laboratory frame is given by[b]

$$E_{CM} = E_\gamma - [E(A) - E(A^-)]$$
$$= E + \frac{m}{M}W - 2(mEW/M)^{1/2}\cos\phi, \tag{10}$$

where E_{CM} = center-of-mass electron energy, E_γ = photon energy, $E(A) - E(A^-)$ = energy difference between the neutral and ion state of the investigated transition, m = electron mass, M = ion mass, E = laboratory electron energy, and W = ion kinetic energy. In the subsequent discussion we assume that the electron center-of-mass velocity exceeds the ion velocity, so that ϕ can take values between 0° and 180°.

The Doppler energy width for photodetached electrons, which are detected at right angles to the ion beam ($\phi = 90°$) with an effective acceptance angle (including ion beam divergence) of $\Delta\phi$, is given to a good approximation by

$$\Delta E_D(90°) \approx 2(mEW/M)^{1/2}\Delta\phi. \tag{11}$$

For the experiments of Breyer *et al.*,[76,77] $Wm/M \approx 5$ meV, $\Delta\phi \approx 0.025$ rad, yielding $\Delta E_D = 3.5$ meV at $E = 1$ eV, i.e., the Doppler energy spread contributed to the effective resolution at a comparable level as did the spectrometer itself. As discussed earlier, electron detection parallel ($\phi = 0°$) or antiparallel ($\phi = 180°$) to the ion beam direction will be more favorable[52,53,77] with respect to kinematic broadening. This

[b] Note the error in Eq. (10) of the 1975 review (Ref. 1), where cos ϕ was replaced by sin ϕ.

effect, however, can also be alleviated by decreasing the ion beam energy.

The electron energy width associated with the ion energy spread is given by

$$\Delta E(\Delta W;\phi = 0°,\ 180°) = [(m/M) \mp (mE/MW)^{1/2}]\Delta W, \tag{12}$$

where the minus sign corresponds to $\phi = 0°$. The broadening due to the finite acceptance angle $\Delta\phi$ (including ion beam divergence) is

$$\Delta E(\Delta\phi;\phi = 0°,\ 180°) = (mEW/M)^{1/2}\Delta\phi^2/4. \tag{13}$$

For a 4-keV O^- beam with $\Delta W = 1$ eV and an acceptance angle $\Delta\phi = 0.03$, one finds at $E = 1$ eV: $\Delta E(\Delta W) = (3.4 \mp 9.2)\times 10^{-5}$ eV, $\Delta E(\Delta\phi) = 8.3\times 10^{-5}$ eV. These widths are negligible compared with any present dispersive electron energy spectrometer resolution. To our knowledge, "coaxial" electron detection has not been used so far in photodetachment experiments, although it clearly presents a possible alternative.[52,53] The basic problem remaining, however, is to improve the resolution of electron energy analyzers to better than 1 meV. We note that the energy width of the cw Ar- and Kr-ion lasers, mainly used in photodetachment electron spectrometry so far, enters at the 10^{-4} eV level.

4. Laser Photodetachment Threshold Studies of Atomic Negative Ions

The determination of electron affinities is accomplished by measuring the threshold photon frequency of the transition from the negative ion ground state to the ground state of the neutral atom plus a threshold electron (zero energy in center-of-mass frame). Sometimes it may be favorable to measure the onset due to the formation of an excited state of the neutral and subtract the (normally accurately known) excited state energy. Assuming that the observed transition is identified without ambiguity, the determination of the threshold position from the frequency dependence of the detachment product rate involves only an extrapolation based on a known threshold law; this extrapolation is especially true in cases where one tries to determine the threshold within a fraction of the effective resolution.

4.1. Threshold Laws

According to Wigner,[22] the leading term in the energy dependence of the photodetachment cross section near threshold is given by

$$\sigma_L = a(\nu - \nu_{thr})^{L+1/2} = bE^{L+1/2}, \tag{14}$$

where ν = laser frequency, ν_{thr} = threshold frequency, E = (center of mass) electron energy, and a,b = constants.

The Wigner law [Eq. (14)] has been found to be a good description of the experimental cross-section behavior over a few meV above threshold for several cases of s-wave detachment ($L = 0$)[38,39] and p-wave detachment ($L = 1$).[40,57,66] In some systems, however, the range of validity is distinctly narrower (e.g., for excited state onsets in alkali ion detachment) and influenced by the presence of resonances.[41,67,69,70] Therefore, a careful study of the threshold of interest precedes the derivation of the electron affinity with an accuracy comparable to the effective resolution of the experiment. Detailed discussions of the threshold behavior of the photodetachment cross sections for atomic negative ions can be found in the literature.[38–40,57]

4.2. Experiments Using Crossed Ion and Laser Beams

The pulsed dye laser crossed-beam apparatus[38,41] used in the early work at JILA has been described in our 1975 review.[1] With this device, the electron affinities of the atoms P, S, K, Se, Rb, Te, Cs, Pt, and Au have been determined with accuracies of 0.2–2 meV. Feldmann has used an optical parametric oscillator laser system to study the thresholds of H^-,[66] Li^-,[57] C^-,[58] and P^-,[57] in the infrared region, yielding EA's with uncertainties $\leqslant 0.5$ meV (2 meV for H). As an example, Fig. 1 presents his results for Li^-, corresponding to a p-wave threshold. Multimode cw dye lasers have been subsequently used by Slater *et al.*,[67] by Frey *et al.*,[69,70] and by Geballe *et al.*[71,72] in studies of the total and partial photodetachment cross sections of K^-, Rb^-, and Cs^- in the vicinity of the lowest neutral excited state thresholds. Slater *et al.*[67] employed a special threshold electron detector to measure the cross sections for excited state formation, whereas Geballe *et al.*[71,72] detected the alkali resonance fluorescence. In a study of Rb^-, Frey *et al.*[69,70] used a high-pass electron energy filter to measure the neutral ground state Rb(5s) cross section separately; in conjunction with the simultaneously sampled total cross section they could also accurately determine the excited state Rb($5p_{1/2}$) cross section and its threshold to within 20 μeV. This uncertainty is close to what can be achieved in a crossed-beams threshold experiment.[51,68,70]

A series of H^- photodetachment experiments has been carried out by Bryant *et al.*[80–82] using a relativistic (800 MeV) H^- beam. Relativistic time dilation and Doppler tuning by varying the angle between the H^- beam and the laser beam [see Eq. (5)] enabled them to study the photodetachment of H^- at energies around the H($n = 2$) threshold and above. Their work gave direct information on H^- photoabsorption resonances associated with H($n = 2,3$)[80,81] and also made a contribution to the theshold behavior of double photode-

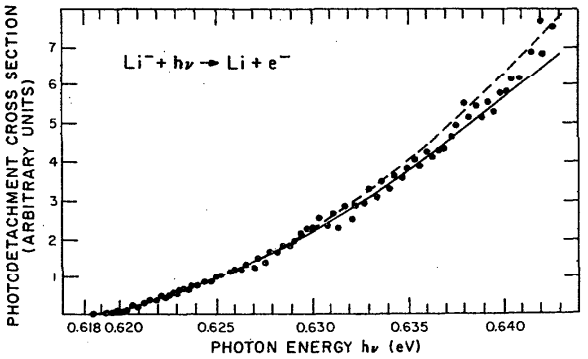

FIG. 1. Threshold photodetachment cross section for Li^- ions. These data were obtained in a crossed laser-ion beam experiment with a resolution of 0.5 meV. The solid lines represent theoretical fits to the p-wave threshold cross section. (Reprinted from Ref. 57, with permission.)

tachment.[82] The overall accuracy of threshold detemina-tions is in the meV range, i.e., comparable to the infrared threshold study of H^- by Feldmann.[66]

4.3. Coaxial Beam Experiments

A substantial improvement in threshold measurements came with the application of the coaxial ion-laser beam technique.[49,51] The apparatus used at JILA is shown in Fig. 2. The well-collimated negative ion beam and the coaxial output of a stabilized single mode ring dye laser interact over a distance of about 30 cm. Neutral atoms are detected downstream via electron emission from an optically transparent, electrically conductive plate (KDP); threshold electrons are magnetically confined and guided to the detecting electron multiplier. The background density in the interaction region is approximately $10^7/cm^3$. This apparatus has demonstrated an effective resolution of 12 MHz in a study of C_2^--autodetachment resonances.[51] Special care was required to reduce the ion source energy spread to ≈ 0.1 eV.

For the determination of electron affinities, the threshold electron detector is particularly useful, since it affords discrimination against photodetachment signals from channels which opened at lower photon energies, and also against a large fraction of the collisional detachment background. Therefore, the sensitivity for threshold studies is increased substantially beyond the limits discussed in Sec. 3.3. For a precise determination of the electron affinity, two independent measurements are carried out with the laser beam parallel (↑↑) and antiparallel (↑↓) to the ion beam direction. In this way, two different apparent threshold laser frequencies $\nu_0^{\uparrow\uparrow}$ and $\nu_0^{\uparrow\downarrow}$ are obtained, which are related to the true threshold frequency ν_{thr} by

$$\nu_{thr} = \frac{\nu_0^{\uparrow\uparrow}(1 - v/c)}{[1 - (v/c)^2]^{1/2}} = \frac{\nu_0^{\uparrow\downarrow}(1 + v/c)}{[1 - (v/c)^2]^{1/2}}, \tag{15}$$

where v is the ion velocity. Taking the average of $\nu_0^{\uparrow\uparrow}$ and $\nu_0^{\uparrow\downarrow}$, the first-order Doppler effect is eliminated, and the threshold frequency is calculated from

$$\nu_{thr} = \frac{(\nu_0^{\uparrow\uparrow} + \nu_0^{\uparrow\downarrow})[1 - (v/c)^2]^{1/2}}{2}. \tag{16}$$

As an example, Fig. 3 presents recent threshold data[83] on the $^{16}O^-(^2P_{3/2}) \rightarrow {}^{16}O(^3P_2)$ electron affinity transition. Hyperfine structure is absent here, but in cases with nuclear spin, it would have to be taken into account at this resolution. The evaluation of the data in Fig. 3 yields $\nu_{thr}(O) \hat{=} 11\,784.645(8)\ cm^{-1}$.[83] The second-order Doppler term, taken into account, amounts to 2.15×10^{-7} (0.0025 cm^{-1}). To date, the JILA coaxial beam machine has been used to

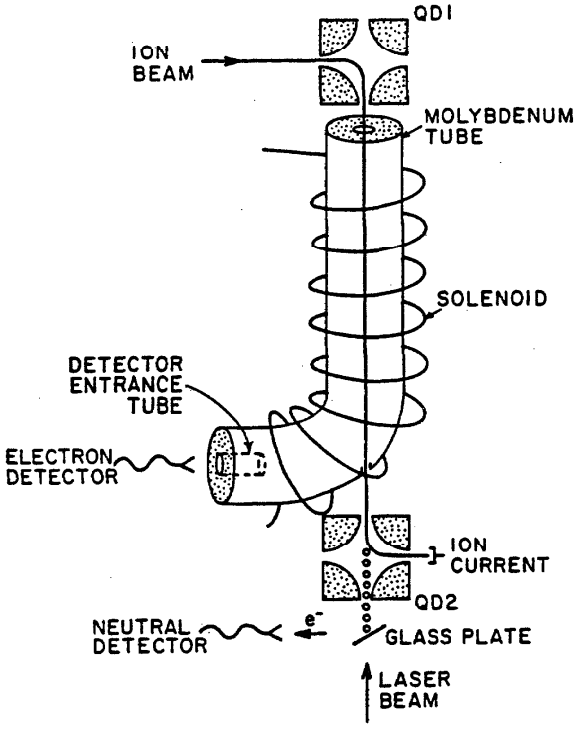

FIG. 2. View of ion beam deflectors, electron collection, and particle detection devices used in the JILA coaxial beam photodetachment apparatus. The entire region shown is enclosed in magnetic shielding and is pumped to below 10^{-9} Torr. The mass selected ion beam enters from the upper left while the single mode dye laser beam enters from the bottom of the figure. Quadrupole deflectors QD1 and QD2 are used to merge the ion beam with the laser beam [R. D. Mead, K. R. Lykke, W. C. Lineberger, J. Marks, and J. I. Brauman, J. Chem. Phys. **81**, 4883 (1984), with permission].

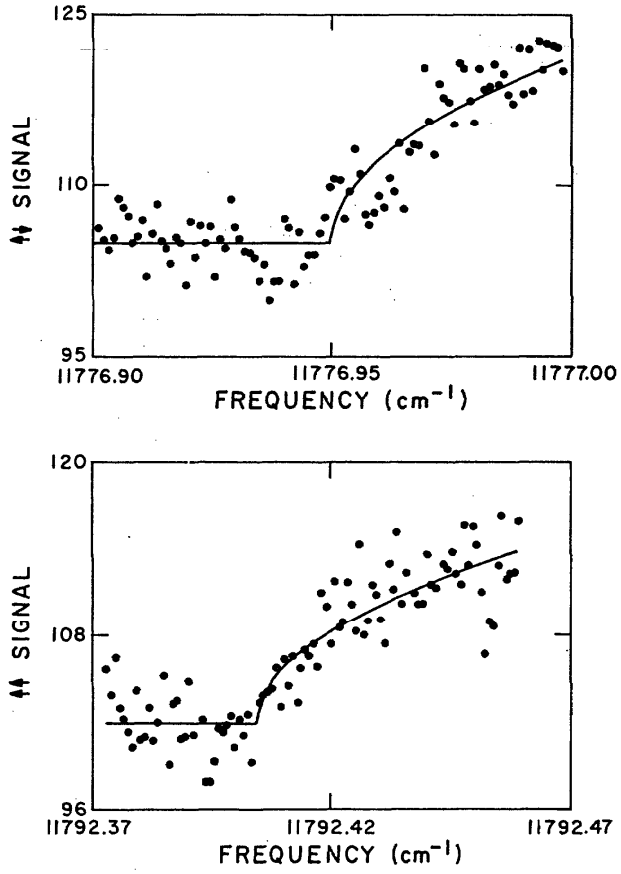

FIG. 3. Ultrahigh resolution view of the $O^-(^2P_{3/2}) \rightarrow O(^3P_2) + e$ photodetachment threshold obtained with the JILA coaxial beam machine. The lower figure corresponds to ion and laser beams propagating in the same direction, while the upper figure corresponds to counterpropagation. See text for details of the analysis. (Reprinted from Ref. 83, with permission.)

study the threshold photodetachment of O^- (Ref. 83) and S^- (Ref. 84) atomic negative ions. The latter study utilized Doppler (energy) tuning of the ion beam to scan the threshold region.

Another apparatus[49] of this type, constructed earlier and used previously for photodissociation experiments of positive and negative ions, has been applied to study photodetachment of stable and metastable ions by Peterson *et al.*[31,65,85,86] They investigated in detail the total photodetachment cross section of $He^-(1s2s2p\ ^4P^\circ)$ around the $He(1s2p\ ^3P)$ threshold[19,65,85] and that of $Li^-(2s^2\ ^1S_0)$ around the $Li(2p\ ^2P)$ threshold.[86] In both cases, careful analysis of the experimental data using modified threshold laws yielded *EA*'s with an uncertainty below 1 meV {*EA* [$He(2^3S)$] = 77.4(8) meV; *EA* [$Li(2s)$] = 0.6173(7) eV}.

4.4. Photodetachment of Trapped Ions

The interaction of photons with ions stored in electromagnetic traps provides an alternative to the crossed or coaxial beam techniques for studies of photon processes under collision-free conditions. Several groups have utilized ion cyclotron resonance spectrometers to investigate the photodestruction of trapped negative ions,[4,8,73] which are normally produced by electron impact from a suitable gaseous sample. The concentration of a particular negative ion species is obtained by monitoring the radio frequency power absorbed from a marginal oscillator (or other detector) tuned to the cyclotron resonance frequency of that ion. An advantage of this method is the possibility of cooling the ions to a near thermal distribution prior to irradiation. This aspect is of particular use in the study of molecular ions. Janousek and Brauman[4] and Drzaic, Marks, and Brauman[8] have given very detailed reviews of such photodetachment studies of molecular negative ions.

For atomic negative ions, the method of trapped ions has only been applied in the interesting work by Larson *et al.*,[74,87] who used a Penning ion trap to study photodetachment of S^- ions in a strong magnetic field (0.7–1.5 T). They employed[87] a single mode ring dye laser to illuminate a cloud of ions at a background pressure of $\sim 10^{-9}$ Torr. They measured the depletion of the stored ions by detecting the image current induced on the ring electrode of the Penning trap as a result of the axial ion motion, driven by a suitable rf field applied to the end caps of the trap. The Doppler limited linewidth is about 3 GHz. At each laser frequency, a measurement cycle of about 30 s is carried out, consisting of filling the trap by dissociative electron attachment to OCS, followed an interval for pump down, the determination of the ion number, a photodetachment period, another measurement of the ion number, and emptying the trap. In this way, a threshold photodestruction curve is created, from which the threshold frequency may be located within about $\pm$ 0.6 GHz (0.02 cm^{-1}). The magnetic field has a non-negligible influence on the location of the photodetachment threshold and on the threshold behavior. Due to the zero point energy of the detached electron in the magnetic field, the apparent threshold energy rises with increasing magnetic field. In the range 0.75–1.5 T, Larson and Stoneman[87] found a linear relation with a slope of 0.494(24) cm^{-1}/T for $^{32}S^-(^2P_{3/2})$ detachment. Extrapolation to zero magnetic field yielded the electron affinity by *EA* (S) = 16 752.967(29) cm^{-1} in remarkable agreement with the value *EA* (S) = 16 752.966(10) cm^{-1} from recent coaxial beam data.[84] Their work now provides[126] the best value for *EA* (Se). There are some questions left[87] concerning the weighting of the various unresolved Zeeman thresholds and differences between photodetachment with π and σ polarizations. Future studies with ions cooled to low temperatures, and the application of higher magnetic fields appear very promising.

4.5. Experiments Exploiting the Optogalvanic Effect

Spectroscopy of atoms, molecules, and ions can be done in a discharge by exploiting the laser optogalvanic (LOG) effect.[88,89] When a laser is tuned to a spectral region in which species in the discharge absorb, this absorption may cause a change in the discharge current, which can be easily detected (see, for example, Goldsmith and Lawler[88] for a recent review). Webster and colleagues[90,91] and Klein and Leone[92] have demonstrated that LOG photodetachment studies of negative ions are feasible and useful for rather accurate *EA* determinations. Basically, photodetachment causes an increase in the discharge current due to the higher mobility of the electrons (the negative ion densities are comparable to the free electron density). To date, Webster *et al.*[90,91,93] have carried out LOG studies of the photodetachment threshold of I^-,[90] Cl^-,[91] and Br^- [91,93]; Klein and Leone[92] photodetached the molecular ion CN^-. Webster *et al.*[90,91] used a pulsed laser with a bandwidth of 0.01 nm (0.6 cm^{-1}) and determined the threshold energies with an uncertainty in the 0.1–1 meV range. Figure 4 shows their result for the $I^-(^1S_0) \rightarrow I(^2P_{3/2})$ threshold.[90]

Webster *et al.*[90,91] discuss in some detail the possible broadening and/or shifting of the photodetachment threshold due to electric fields in the discharge and have come to the conclusion—also in view of the perfect agreement of their I^- result with the early beam data of Steiner *et al.*[94]—that such effects are negligible, at least at the meV level, and

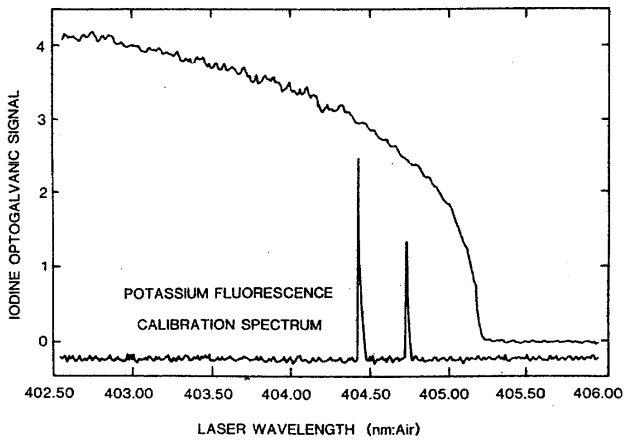

FIG. 4. The I^- photodetachment optogalvanic spectrum near the photodetachment threshold. The upper trace is the optogalvanic signal, while the lower trace is a laser induced fluorescence spectrum of atomic potassium used for calibration. (Reprinted from Ref. 90, with permission.)

probably below. A precise EA determination at least for the iodine atom with the coaxial laser beam method would be desirable in order to permit the definite conclusion that the LOG photodetachment thresholds are unperturbed at the 10^{-4} eV level.

5. Laser Photodetached Electron Spectrometry Studies of Atomic Negative Ions

5.1. Introduction

Laser photodetached electron spectrometry using intense fixed frequency cw ion lasers has so far provided the majority of atomic EA determinations.[42,45,46,62–64,95–97] Typical uncertainties range between 2 and 20 meV. LPES may be employed for any atoms with EA's between zero and the energy of the photons used. When one uses the 351.1-nm (3.53-eV) Ar^{++} laser line, all atomic negative ions except Cl^- can be photodetached. In most cases, the much more intense 488-nm (2.54-eV) Ar^+ laser line suffices.

For systems with several accessible negative ion and neutral atom states (e.g., due to fine structure) a multiline electron spectrum will result. Comparison of the measured line intensities with theoretical predictions[96–102] and also electron angular distribution[42,45,46,76,77,96] studies may significantly help to understand such a spectrum and unambiguously identify the electron affinity transition.

Studies of the transition metal negative ions[62,64,96,97] provide illustrative examples of some of the complications that may be encountered. For transitions between various fine-structure states of the negative ion (total angular momentum J'') and the neutral (J'), line intensities are frequently found[38,39,76,96,97] to be in good agreement with "geometrical factors."[96,98–101] For $J''\rightarrow J'$, transitions between LS-coupled states the relative intensities are given by[96,100,101]

$$I(J',J'') = f(J'')\sum_{j=l-1/2}^{j=l+1/2}(2J'+1)(2J''+1)(2j+1)\begin{Bmatrix} S'' & L'' & J'' \\ 1/2 & l & j \\ S' & L' & J' \end{Bmatrix}, \tag{17}$$

where l is the orbital angular momentum of the detached electron and S, L, J are the usual spin, orbital, and total angular momentum quantum numbers. $f(J'')$ is a function which describes the *deviation* of the negative ions J''-level population from the statistical $(2J''+1)$ value. For a negative ion source with infinite temperature $f(J'')\equiv 1$.

5.2. Crossed Beams LPES Experiments with Electron Detection Perpendicular to the Ion Beam

All LPES machines constructed to date[42,43,76,77,78,103–105] have used the same principle: a mass-selected negative ion beam crosses the focal waist of a cw Ar-ion laser (inside the cavity), and the electrons photodetached into a narrow cone perpendicular to both the ion and laser beams are energy analyzed with an electrostatic condenser. As pointed out in Sec. 3.4.b, this choice is not the best from the standpoint of minimal kinematic broadening. It is, however, practical (especially regarding the discrimination of background due to collisional detachment), and at an electron energy resolution $\gtrsim 10$ meV, the first-order Doppler broadening can be made to be negligible.

Due to contact potential differences and other problems with precise determination of the absolute electron energy scale, the measurement of an electron affinity of some atom A_2 is carried out by comparison with the known electron affinity of a reference atom A_1.[1,42–44] For this purpose, a mixed ion beam of A_1^- and A_2^- is simultaneously exposed to photodetachment, and $EA(2)$ is calculated from the basic working equation [see also Eq. (10)]:

$$EA(2) = EA(1) + (E_1 - E_2) + mW\left(\frac{1}{M_1} - \frac{1}{M_2}\right). \tag{18}$$

Here, $(E_1 - E_2)$ is the difference between the electron energies for those two peaks, which correspond to the respective electron affinity transitions.

If the average electron detection angle deviates from $\phi = 90°$, Eq. (16) is modified to include a term $-2(mW)^{1/2} \times[(E_1/M_1)^{1/2} - (E_2/M_2)^{1/2}]\cos\phi$ on the right side. By comparing energies of transitions from the same ion state to different known states of the neutral atom, the presence of this ϕ-dependent term can be checked and taken into account.[77] The observation of an energy scale compression factor, as noted in work with the first JILA apparatus,[42,46,62,64,96,97] may at least in part be related to this term.

The first LPES apparatus, built in 1966 by Brehm, Gusinow, and Hall[42] at JILA and later refined and used by Lineberger *et al.*[45,46,62–64,95–97] for about 15 years, so far has produced the majority of atomic EA determinations. A hemispherical condenser with a virtual entrance slit was used for electron energy analysis with a resolution of 50–60 meV. As an illustrative example, we briefly discuss LPES of Pd^-, as reported by Feigerle *et al.*[62] A 680-eV, 15-pA beam of Pd^- ions from a sputter ion source interacted with a 488-nm cw Ar-ion laser inside the cavity (power about 100 W), giving the electron energy spectrum shown in Fig. 5. Contributions from small amounts of PdH^- in the ion beam have been subtracted. The spacings between peaks B, D, E,F, and H were found to agree within 3 meV with the separations between the five lowest atomic states, as shown in the level diagram. The spacings between peaks A, C, D, and G agree with the separations between the neutral states $^1S_0$, $^3D_3$, $^3D_2$, and $^1D_2$ within 7 meV. The spectrum therefore signals the presence of two bound negative ion states, separated by the (identical) spacings A–B, C–D, D–E, G–H of about 0.14 eV. Possible negative ion states are $Pd^-(4d^{10}5s)^2S_{1/2}$, $Pd^-(4d^9 5s^2\ ^2D_{1/2})$, and $Pd^-(4d^9 5s\ ^2D_{3/2})$. In view of an expected $^2D_{5/2}$–$^2D_{3/2}$ splitting of 0.43(5) eV, as

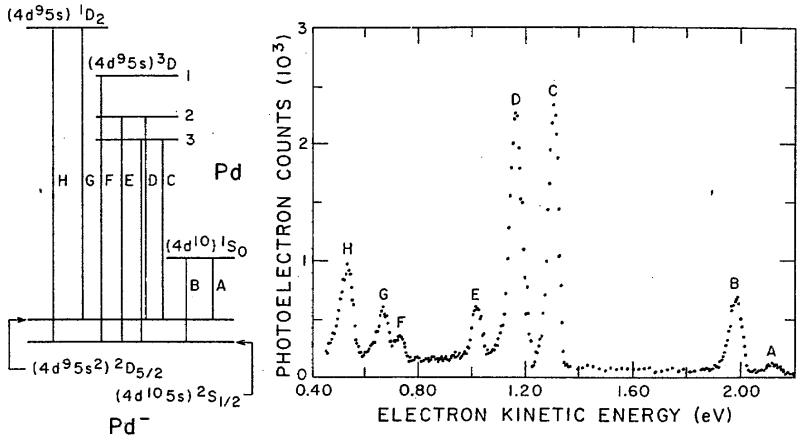

FIG. 5. The 488-nm photoelectron spectrum of Pd^- and relevant atomic energy levels. The lettered peaks in the spectrum are assigned to the equivalently lettered transitions indicated in the energy level schematic. Peak B corresponds to the *EA* (Pd) defining transition. (Taken from Ref. 62, with permission).

predicted by isoelectronic extrapolation, the two states in question are $^2S_{1/2}$ and $^2D_{5/2}$. On the basis of selection rules for single electron detachment, one expects the transition from $Pd^-(4d^95s^2\ ^2D_{5/2})$ to $Pd(4d^95s\ ^3D_1)$ to be missing (or at least very weak); therefore, the sequence of only four peaks A,C,D,G is associated with $Pd^-(^2D_{5/2})$. Since these four peaks lie at higher electron energies than the other peak sequence, the $Pd^-(^2D_{5/2})$ level lies above $Pd^-(^2S_{1/2})$, the latter being the ground state of the negative ion with a binding energy of 0.558(8) eV. Cases more complicated than Pd^- have been studied and the reader is referred to the original papers[62,64,96,97] for an appreciation of the problems involved.

The apparatus constructed by Breyer *et al.*[76,77] uses a hemispherical analyzer ($R = 5$ cm) with two real slits (0.5 mm) and some special steering electrodes. With fixed intracavity laser focus, the whole analyzer can be translated parallel to the ion beam. In this way, the effective electron detection angle ϕ and the angular acceptance $\Delta\phi$ can be easily varied, a feature which was found important to achieve a resolution of 5 meV in studies of O^-, S^-, OH^-, SH^-, and SD^-.

Figure 6 shows a high-resolution O^- spectrum, reported by Breyer *et al.*[76,77] It was measured at an analyzer pass energy of 0.6 eV with the 488-nm Ar-ion laser line and a 180-eV O^- beam. The separate solid curves show the individual fine-structure transitions, determined by a least-squares fit to the data points. The relative intensities[76] agree well with the relevant *LS*-geometrical factors [Eq. (17)], and the $O^-(^2P)$ spin-orbit splitting was determined to be 22.0(2) meV [177.4(16) cm^{-1}],[76] in excellent agreement with the more precise value obtained in the very recent LPT study[83] with the JILA coaxial beam machine.

The O^- spectrum is of particular interest since it has served in most *EA* measurements for calibration of the energy scale [Eq. (18)]. Until recently, the value $EA(O)_{eff} = 1.465(3)$ eV[1] has been used for the *effective* electron affinity of oxygen, which corresponds to the center of gravity of all the fine-structure transitions, i.e., the peak location in low-resolution spectra. With the new value $EA(O) = 1.4611$ eV the effective value is reduced by 1 meV. Consequently, all previous *EA* values, determined relative to O^-, have been reduced by 1 meV. Note that the effective $EA(O)_{eff}$ depends on the relative population of the $O^-(^2P)$ fine structure states. At ion source temperatures of 0/300/1000/10^4 K, $EA(O)_{eff}$ is larger than $EA(O)$ by 6.5/4.3/3.0/2.4 meV. The previous value had been chosen to correspond to $T \approx 1000$ K, and $EA(O) = 1.462(3)$ eV was the value recommended in 1975.[1]

To our knowledge, two further LPES machines have recently come into operation. Ellison *et al.*[105] use a two-stage

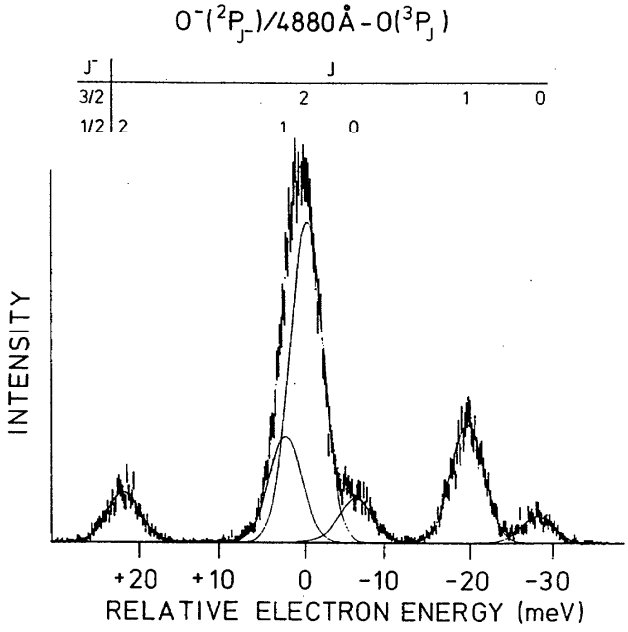

FIG. 6. The 488-nm photoelectron spectrum of O^- ions. The various fine-structure transitions are identified above the spectrum, and the energy scale is in meV, relative to the $O^-(^2P_{3/2}) \rightarrow O(^3P_2)$ transition. The resolution is 4.7 meV. (Taken from Ref. 76, with permission.)

hemispherical analyzer with a typical resolution of 20 meV; their work is dedicated to LPES of organic anions. Bowen *et al.*[106] use a single hemispherical analyzer at a resolution of $\approx$20 meV to study negative cluster ions such as Te_n^-.

At JILA, a new hemispherical analyzer with multichannel detection[78,103] has recently replaced the old one. Both the sensitivity and the resolution have been substantially improved. The new spectrometer, designed by Feigerle,[106] is shown in Fig. 7. Its performance is demonstrated in Fig. 8, which presents the electron spectrum of W^-,[78,106] photodetached at 488 nm. At the 5–12 meV resolution of this device, the reference O^- fine-structure transitions are resolved, and there is no longer a need to employ an effective *EA* (O). With a cold, flowing afterglow ion source, this new device offers the promise of precise *EA* determinations for the lanthanides and actinides.

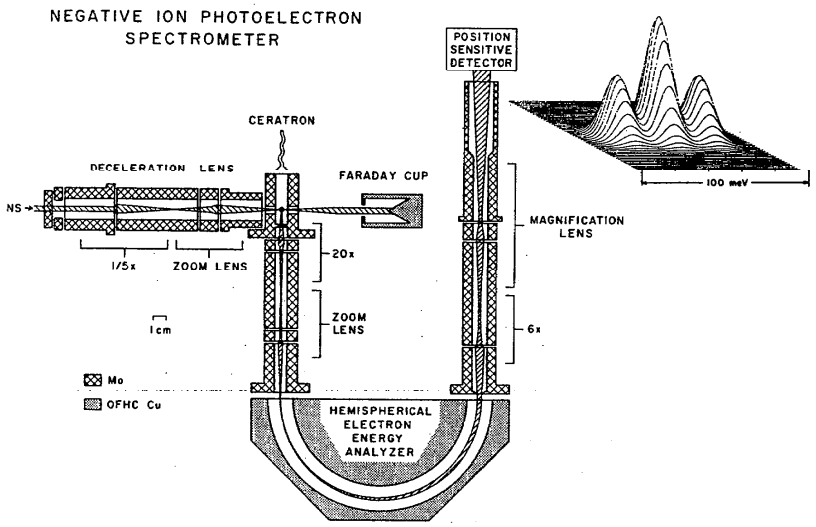

FIG. 7. Interaction region of the new high sensitivity negative ion photoelectron spectrometer. Ion deceleration, larger aperture electron optics, and multichannel detection improve the sensitivity by nearly three orders of magnitude over the earlier devices. (Taken from Ref. 106, with permission).

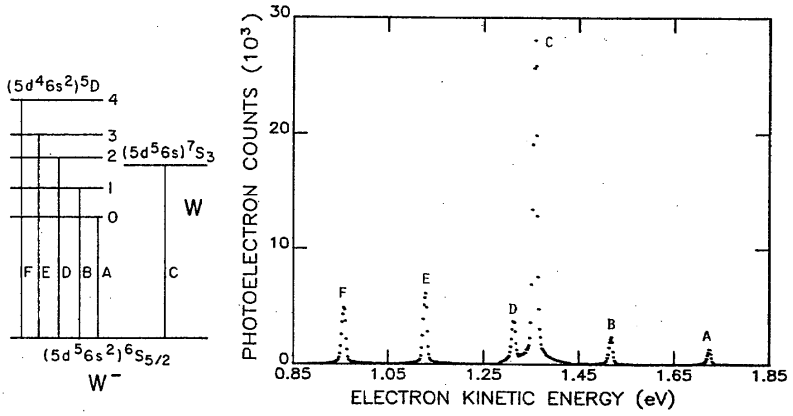

FIG. 8. The 488-nm photoelectron spectrum of W^- ions obtained with the spectrometer depicted in Fig. 7. The relevant energy level diagrams and observed transitions are indicated. The resolution here is approximately 10 meV. (Taken from Ref. 106, with permission.)

6. Recommended Values for Atomic Electron Affinities

Table 1 presents those values of atomic electron affinities ($Z \leqslant 86$) which we recommend as being the most reliable. In each case, we have listed the atomic charge Z, the parent atom state, the relevant negative ion state, the EA, including its present uncertainty, the method(s) of determination, and the respective references. If different methods have yielded EA's with comparable accuracy, the listed EA represents either a weighted average or our preferred value. In several cases, the reported error bars represent our judgment, rather than that in the original reference. As in 1975, we have omitted the lanthanide atoms ($Z = 58$–71), but we refer the reader to the papers by Bratsch[36] and Cole and Perdew,[33] who have given EA values with an estimated uncertainty of ± 0.3 eV.

A comparison of the present EA's with those in Table 10 of the 1975 review paper shows substantial changes (outside the 1975 uncertainty) in only three cases: Sc, Y, and Pb. For Sc and Y, the negative ion ground state was found to have a different configuration with larger stability. For Pb, there were two possible interpretations of a photodetachment threshold experiment and our choice of the higher of two possible values[54,59] was later shown to be wrong by LPES.[63]

The electron affinities have been given in eV. We note, however, that in threshold experiments, wavelengths and energies are determined in units of vacuum wavenumbers. We have used the conversion 1 eV $\doteq$ 8065.479 cm^{-1}. This conversion has a relative uncertainty of 2.6×10^{-6} which we have not included. The additional uncertainty is only relevant in the few cases (oxygen, sulfur) in which the electron affinity is known with higher accuracy in cm^{-1}. Finally these data are summarized in periodic charts shown in Figs. 9 and 10.

^{1}H 0.754209							^{2}He 0
^{3}Li 0.6180	^{4}Be <0	^{5}B 0.277	^{6}C 1.2629	^{7}N <0	^{8}O 1.4611215	^{9}F 3.399	^{10}Ne <0
^{11}Na 0.54793	^{12}Mg <0	^{13}Al 0.441	^{14}Si 1.385	^{15}P 0.7465	^{16}S 2.077120	^{17}Cl 3.617	^{18}Ar <0
^{19}K 0.50147	^{20}Ca <0	^{31}Ga 0.3	^{32}Ge 1.2	^{33}As 0.81	^{34}Se 2.02069	^{35}Br 3.365	^{36}Kr <0
^{37}Rb 0.48592	^{38}Sr <0	^{49}In 0.3	^{50}Sn 1.2	^{51}Sb 1.07	^{52}Te 1.9708	^{53}I 3.0591	^{54}Xe <0
^{55}Cs 0.47163	^{56}Ba <0	^{81}Tl 0.2	^{82}Pb 0.364	^{83}Bi 0.946	^{84}Po 1.9	^{85}At 2.8	^{86}Rn <0

FIG. 9. Periodic table showing recommended electron affinities for the main group elements. If the negative ion is not stable, then <0 is indicated. Negative ion excited state information is not shown here. For more details, the reader should consult Table 1.

^{20}Ca <0	^{21}Sc 0.188	^{22}Ti 0.079	^{23}V 0.525	^{24}Cr 0.666	^{25}Mn <0	^{26}Fe 0.163	^{27}Co 0.661	^{28}Ni 1.156	^{29}Cu 1.228	^{30}Zn <0
^{38}Sr <0	^{39}Y 0.307	^{40}Zr 0.426	^{41}Nb 0.893	^{42}Mo 0.746	^{43}Tc 0.55	^{44}Ru 1.05	^{45}Rh 1.137	^{46}Pd 0.557	^{47}Ag 1.302	^{48}Cd <0
^{56}Ba <0	^{57}La 0.5	^{72}Hf ≈0	^{73}Ta 0.322	^{74}W 0.815	^{75}Re 0.15	^{76}Os 1.1	^{77}Ir 1.565	^{78}Pt 2.128	^{79}Au 2.30863	^{80}Hg <0

FIG. 10. Recommended electron affinities for the three long series. If the negative ion is not stable, then <0 is indicated. Negative ion excited state information is not shown here. For more details, the reader should consult Table 1.

In addition to the ground and bound electronically excited states listed in Table 1, many atomic negative ions have spin-orbit excited states which are also bound. The number of such systems for which quantitative data are available has increased substantially since 1975. The presently known quantitative fine-structure separations are listed in Table 2. These include both extrapolated and measured fine-structure separations. The major experimental additions to this list are LPES determinations of fine structure in transition metal negative ions.

There is another class of long-lived atomic negative ions, when the extra electron is bound relative to an *excited* metastable state of the neutral. The best known of such systems is He^- ($1s2s2p\ ^4P^\circ$), bound by 77 meV with respect to He $2\ ^3S$. This ion has a μs lifetime, more than adequate to utilize in beam experiments. Table 3 summarizes our knowledge of such metastable negative ion states. The principal criterion for inclusion in this table is a relatively definitive experimental detection of the ion in beam experiments. Only for He^- is there an accurate experimental binding energy, while for Be^-, Mg^-, and Ca^- the calculations are likely to be relatively accurate.

Finally, a decade ago the subject of doubly charged atomic negative ions was a lively topic in the literature.[107–109] It now appears likely that all of these observations were in fact artifacts.

In summary, the state of our knowledge of atomic negative ion binding energies has improved considerably in the last decade. At present only electron affinities of the lanthanides and actinides are completely unknown. The accuracy of some electron affinities (0.006 cm^{-1}) now rivals that of the best known ionization potentials. It is now possible to determine EA (H) to a level (better than 0.01 cm^{-1}) that provides a challenge to theorists. We hope these questions will be answered in a future review.

Table 1. Summary of recommended atomic electron affinities (eV).

Z	Atom	Negative ion state[a]	EA(eV)	Method[b]	Ref.
1	H	$1s\ ^2S_{1/2}(F=0)$	$1s^2\ ^1S_0$	0.754209(3)	Calc.	20,21,1
2	He	$1s^2\ ^1S_0$		<0	Calc.;SE	14,17;1,34
3	Li	$2s\ ^2S_{1/2}$	$2s^2\ ^1S_0$	0.6180(5)	LPT	57,86
4	Be	$2s^2\ ^1S_0$		<0	Calc.;SE	17,111,112;34
5	B	$2p\ ^2P_{1/2}$	$2p^2\ ^3P_0$	0.277(10)	LPES(O^-)	63
6	C	$2p^2\ ^3P_0$	$2p^3\ ^4S_{3/2}$	1.2629(3)	LPT	58
			$2p^3\ ^2D(m)$	0.033(1)	LPT	58
7	N	$2p^3\ ^4S_{3/2}$	$2p^4\ ^3P$	-0.07(2)	Diss. Att.	113
8	O	$2p^4\ ^3P_2$	$2p^5\ ^2P_{3/2}$	1.4611215(10)	LPT	83
9	F	$2p^5\ ^2P_{3/2}$	$2p^6\ ^1S_0$	3.399(3)	PℓE;PℓA	114;115
10	Ne	$2p^6\ ^1S_0$		<0	Calc.;SE	17;34
11	Na	$3s\ ^2S_{1/2}$	$3s^2\ ^1S_0$	0.547930(25)	LPT	116
12	Mg	$3s^2\ ^1S_0$		<0	Calc.;e^- scatt.	17,111;123
13	Aℓ	$3p\ ^2P_{1/2}$	$3p^2\ ^3P_0$	0.441(10)	LPES(O^-)	63
			$3p^2\ ^1D_2(m)$	0.109(10)	LPES(O^-)	63
14	Si	$3p^2\ ^3P_0$	$3p^3\ ^4S_{3/2}$	1.385(5)	LPES(K^-)	95
			$3p^3\ ^2D_{3/2,5/2}(m)$	0.523(5)	LPES(K^-)	95
			$3p^3\ ^2P_{1/2,3/2}(m)$	0.029(5)	LPES(K^-)	95
15	P	$3p^3\ ^4S_{3/2}$	$3p^4\ ^3P_2$	0.7465(3)	LPT	57,117
16	S	$3p^4\ ^3P_2$	$3p^5\ ^2P_{3/2}$	2.077120(1)	LPT	84
17	Cℓ	$3p^5\ ^2P_{3/2}$	$3p^6\ ^1S_0$	3.617(3)	LOG;PℓE	91;118
18	Ar	$3p^6\ ^1S_0$		<0	Calc.;SE	17;34
19	K	$4s\ ^2S_{1/2}$	$4s^2\ ^1S_0$	0.50147(10)	LPT	67
20	Ca	$4s^2\ ^1S_0$		<0	Calc.;SE	17;34

Table 1. Summary of recommended atomic electron affinities (eV)--Continued

Z	Atom	Negative ion state[a]	EA(eV)	Method[b]	Ref.
21	Sc $3d4s^2\ ^2D_{3/2}$	$3d4s^24p\ ^1D$ or ^3D	0.188(20)	LPES(O^-)	64
		$3d4s^24p\ ^3D$ or ^1D (m)	0.041(20)	LPES(O^-)	64
22	Ti $3d^24s^2\ ^3F_2$	$3d^34s^2\ ^4F_{3/2}$	0.079(14)	LPES(O^-)	62
23	V $3d^34s^2\ ^4F_{3/2}$	$3d^44s^2\ ^5D_0$	0.525(12)	LPES(O^-)	62
24	Cr $3d^54s\ ^7S_3$	$3d^54s^2\ ^6S_{5/2}$	0.666(12)	LPES(O^-)	62
25	Mn $3d^54s^2\ ^6S_{5/2}$		<0	SE; calc.	1
26	Fe $3d^64s^2\ ^5D_4$	$3d^74s^2\ ^4F_{9/2}$	0.163(35)	LPES(O^-)	96
27	Co $3d^74s^2\ ^4F_{9/2}$	$3d^84s^2\ ^3F_4$	0.661(10)	LPES(O^-)	97
28	Ni $3d^84s^2\ ^3F_4$	$3d^94s^2\ ^2D_{5/2}$	1.156(10)	LPES(O^-)	97
29	Cu $3d^{10}4s\ ^2S_{1/2}$	$3d^{10}4s^2\ ^1S_0$	1.228(10)	LPES(OH^-)	45
30	Zn $4s^2\ ^1S_0$		<0	e^- scatt.;SE	123;34
31	Ga $4p\ ^2P_{1/2}$	$4p^2\ ^3P_0$	0.30(15)	PT;SE	59;1,34
32	Ge $4p^2\ ^3P_0$	$4p^3\ ^4S_{3/2}$	1.2(2)	PT	59
		$4p^3\ ^2D$ (m)	0.4(2)	PT	59
33	As $4p^3\ ^4S_{3/2}$	$4p^4\ ^3P_2$	0.81(3)	PT	60
34	Se $4p^4\ ^3P_2$	$4p^5\ ^2P_{3/2}$	2.02069(3)	LPT	126
35	Br $4p^5\ ^2P_{3/2}$	$4p^6\ ^1S_0$	3.365(3)	P&E;P&A	119;120
36	Kr $4p^6\ ^1S_0$		<0	SE	34
37	Rb $5s\ ^2S_{1/2}$	$5s^2\ ^1S_0$	0.48592(2)	LPT	69
38	Sr $5s^2\ ^1S_0$		<0	SE	34
39	Y $4d5s^2\ ^2D_{3/2}$	$4d5s^25p\ ^1D_2$	0.307(12)	LPES(O^-)	64
		$4d5s^25p\ ^3D_1$ (m)	0.164(25)	LPES(O^-)	64
40	Zr $4d^25s^2\ ^3F_2$	$4d^35s^2\ ^4F_{3/2}$	0.426(14)	LPES(O^-)	62
41	Nb $4d^45s\ ^6D_{1/2}$	$4d^45s^2\ ^5D_0$	0.893(25)	LPES(O^-)	62
42	Mo $4d^55s\ ^7S_3$	$4d^55s^2\ ^6S_{5/2}$	0.746(10)	LPES(O^-)	62

Table 1. Summary of recommended atomic electron affinities (eV)--Continued

Z	Atom	Negative ion state[a]	EA(eV)	Method[b]	Ref.
43	Tc $4d^5 5s^2\ ^6S_{5/2}$	$4d^6 5s^2\ ^5D_4$	0.55(20)	SE	62
44	Ru $4d^7 5s\ ^5F_5$	$4d^7 5s^2\ ^4F_{9/2}$	1.05(15)	SE	62
45	Rh $4d^8 5s\ ^4F_{9/2}$	$4d^8 5s^2\ ^3F_4$	1.137(8)	LPES(O^-)	62
46	Pd $4d^{10}\ ^1S_0$	$4d^{10} 5s\ ^2S_{1/2}$	0.557(8)	LPES(O^-)	62
		$4d^9 5s^2\ ^2D_{5/2}$ (m)	0.421(8)	LPES(O^-)	62
47	Ag $4d^{10} 5s\ ^2S_{1/2}$	$4d^{10} 5s^2\ ^1S_0$	1.302(7)	LPES(O^-)	45
48	Cd $4d^{10} 5s^2\ ^1S_0$		<0	e^- scatt.;SE	123;34
49	In $5p\ ^2P_{1/2}$	$5p^2\ ^3P_0$	0.3(2)	PT;SE	59;1,34
50	Sn $5p^2\ ^3P_0$	$5p^3\ ^4S_{3/2}$	1.2(2)	PT	59
		$5p^3\ ^2D_{3/2}$ (m)	0.4(2)	PT	59
51	Sb $5p^3\ ^4S_{3/2}$	$5p^4\ ^3P_2$	1.07(5)	PT	60
52	Te $5p^4\ ^3P_2$	$5p^5\ ^2P_{3/2}$	1.9708(3)	PT	117
53	I $5p^5\ ^2P_{3/2}$	$5p^6\ ^1S_0$	3.0591(4)	LOG	90
54	Xe $5p^6\ ^1S_0$		<0	SE	34
55	Cs $6s\ ^2S_{1/2}$	$6s^2\ ^1S_0$	0.471630(25)	LPT	67,116
56	Ba $6s^2\ ^1S_0$		<0	SE	1,34
57	La $5d6s^2\ ^2D_{3/2}$	$5d^2 6s^2\ ^3F_2$	0.5(3)	SE	1,35,36
58	Rare earths		$\lesssim$0.5	semiempirical estimate	35,36
71					
72	Hf $5d^2 6s^2\ ^3F_2$	$5d^3 6s^2\ ^4F$	≈0	SE	1,34
73	Ta $5d^3 6s^2\ ^4F_{3/2}$	$5d^4 6s^2\ ^5D_0$	0.322(12)	LPES(O^-)	62
74	W $5d^4 6s^2\ ^5D_0$	$5d^5 6s^2\ ^6S_{5/2}$	0.815(8)	LPES(O^-)	62
75	Re $5d^5 6s^2\ ^6S_{5/2}$	$5d^6 6s^2\ ^5D_4$	0.15(15)	SE;SSI	1,34,62;121
76	Os $5d^6 6s^2\ ^5D_4$	$5d^7 6s^2\ ^4F$	1.1(2)	SE	1,34,62

Table 1. Summary of recommended atomic electron affinities (eV)--Continued

Z	Atom		Negative ion state[a]	EA(eV)	Method[b]	Ref.
77	Ir	$5d^7 6s^2\ ^4F_{9/2}$	$5d^8 6s^2\ ^3F_4$	1.565(8)	LPES(0^-)	62
78	Pt	$5d^9 6s\ ^3D_3$	$5d^9 6s^2\ ^2D_{5/2}$	2.128(2)	LPT	40
79	Au	$5d^{10} 6s\ ^3S_{1/2}$	$5d^{10} 6s^2\ ^1S_0$	2.30863(3)	LPT	40,122
80	Hg	$6s^2\ ^1S_0$		<0	e^- scatt.;SE	124,34
81	Tℓ	$6s^2 6p\ ^2P_{1/2}$	$6p^2\ ^3P_0$	0.2(2)	PT;SE	59;34
82	Pb	$6p^2\ ^3P_0$	$6p^3\ ^4S_{3/2}$	0.364(8)	LPES(0^-)	63
83	Bi	$6p^3\ ^4S_{3/2}$	$6p^4\ ^3P_2$	0.946(10)	LPES(0^-)	63
84	Po	$6p^4\ ^3P_2$	$6p^5\ ^2P_{3/2}$	1.9(3)	SE	34
85	At	$6p^5\ ^2P_{3/2}$	$6p^2\ ^1S_0$	2.8(2)	SE	34
86	Rn	$6p^6\ ^1S_0$		<0	SE	34

Notes for Table 1.

[a](m) indicates metastable.

[b]Abbreviations used:

Calc.	ab initio calculation
PT	Photodetachment threshold using conventional light sources
LPT	Tunable laser photodetachment threshold
LPES	Laser photodetachment electron spectrometry
LOG	Laser optogalvanic spectroscopy
SE	Semiempirical extrapolation (isoelectronic extrapolation and/or horizontal analysis)
PℓA, PℓE	Plasma absorption, plasma emission
SSI	Self-Surface Ionizations
e^- scatt.	Electron scattering resonance
Diss. Att.	Dissociative attachment of electrons

Table 2. Fine-structure separations in atomic negative ions.

Z	Negative ion	Fine-structure interval[a]	Separation (cm^{-1})	Method[b]	Ref.
2	$He^-(1s2s2p\ ^4P^o)$	5/2 → 3/2	0.027508(27)	rf	125
		5/2 → 1/2	0.2888(18)	rf	125
5	$B^-(^3P)$	0 → 1	4(1)	RIE	1
		0 → 2	9(1)	RIE	1
6	$C^-(^2D)$	3/2 → 5/2	3(1)	LIE	1
8	$O^-(^2P)$	3/2 → 1/2	177.08(5)	LPT	83
13	$Al^-(^3P)$	0 → 1	26(3)	RIE	1
		0 → 2	76(7)	RIE	1
14	$Si^-(^2D)$	3/2 → 5/2	7(2)	LIE	1
15	$P^-(^3P)$	2 → 1	181(2)	LPT	57,117
		2 → 0	263(2)	LPT	57,117
16	$S^-(^2P)$	3/2 → 1/2	483.54(1)	LPT	84
22	$Ti^-(^4F)$	3/2 → 5/2	72(7)	LIE	62
		5/2 → 7/2	99(10)	LIE	62
		7/2 → 9/2	124(12)	LIE	62
		3/2 → 9/2	295(15)	LIE	62
23	$V^-(^5D)$	0 → 1	35(4)	RIE	62
		1 → 2	70(7)	RIE	62
		2 → 3	100(10)	RIE	62
		3 → 4	125(13)	RIE	62
		0 → 4	330(17)	RIE	62
26	$Fe^-(^4F)$	9/2 → 7/2	540(50)	RIE	62
		7/2 → 5/2	390(40)	RIE	62
		5/2 → 3/2	270(30)	RIE	62
		9/2 → 3/2	1200(60)	RIE	62
27	$Co^-(^3F)$	4 → 3	910(50)	LPES	97
		3 → 2	650(50)	LPES	97
		4 → 2	1560(50)	LPES	97
28	$Ni^-(^2D)$	5/2 → 3/2	1470(100)	LPES	97

Table 2. Fine-structure separations in atomic negative ions--Continued

Z	Negative ion	Fine-structure interval[a]	Separation (cm^{-1})	Method[b]	Ref.
31	$Ga^-(^3P)$	0 → 1	220(20)	RIE; QIE	1;34
		0 → 2	580(50)	RIE; QIE	1;34
32	$Ge^-(^2D)$	3/2 → 5/2	160(30)	LIE	1
33	$As^-(^3P)$	2 → 1	1100(200)	LIE; QIE	1;34
		2 → 0	1500(200)	LIE; QIE	1;34
		2 → 0	≈1370	PT	60
34	$Se^-(^2P)$	3/2 → 1/2	2279(2)	LPT	39
40	$Zr^-(^4F)$	3/2 → 5/2	250(50)	RIE	62
		5/2 → 7/2	330(70)	RIE	62
		7/2 → 9/2	370(70)	RIE	62
		3/2 → 9/2	950(100)	RIE	62
41	$Nb^-(^5D)$	0 → 1	110(20)	RIE	62
		1 → 2	200(40)	RIE	62
		2 → 3	250(40)	RIE	62
		3 → 4	310(60)	RIE	62
		0 → 4	860(90)	RIE	62
45	$Rh^-(^3F)$	4 → 3	2370(65)	LPES	62
		3 → 2	1000(65)	LPES	62
		4 → 2	3370(65)	LPES	62
46	$Pd^-(^2D)$	5/2 → 3/2[c]	3450(350)	RIE	62
49	$In^-(^3P)$	0 → 1	680(70)	RIE; QIE	1;34
		0 → 2	1550(150)	RIE; QIE	1;34
50	$Sn^-(^2D)$	3/2 → 5/2	800(200)	LIE	1
51	$Sb^-(^3P)$	2 → 1	2700(500)	LIE; QIE	1;34
		2 → 0	3000(500)	LIE; QIE	1;34
		2 → (1,0)	≈2740	PT	60
52	$Te^-(^2P)$	3/2 → 1/2	5008(5)	LPT	117
73	$Ta^-(^5D)$	0 → 1	1070(110)	LPES	62
		1 → 2	1170(120)	LPES	62
		2 → 3[d]	980(200)	RIE	62

Table 2. Fine-structure separations in atomic negative ions--Continued

Z	Negative ion	Fine-structure interval[a]	Separation (cm^{-1})	Method[b]	Ref.
77	$Ir^-(^3F)$	4 → 3	7600(1500)	RIE	62
		3 → 2	4400(900)	RIE	62
		4 → 2	12000(1200)	RIE	62
78	$Pt^-(^2D)$	5/2 → 3/2	10000(1000)	RIE; QIE	40;34

a: total angular momentum of lower (left) and upper fine structure levels are listed

b: Abbreviations used:

rf Radio frequency resonance technique

RIE Isoelectronic extrapolation of ratios of fine structure separations.

LIE Isoelectronic extrapolation from logarithmic plot

QIE Quadratic isoelectronic extrapolation

LPT Tunable laser photodetachment threshold

LPES Laser photodetachment electron spectrometry

PT Photodetachment threshold using conventional light sources

c: J = 3/2 not bound

d: J = 3 not bound

Table 3. Selected metastable states of atomic negative ions

Z	Atom state	Negative ion state	EA(eV)	Method	Ref.
2	He($1s2s\ ^3S$)	$1s2s2p\ ^4P^o$	0.0774(5)	Calc. LPT LPES(H^-,D^-)	14 85 42
4	Be($2s2p\ ^3P$)	$2s2p^2\ ^4P^e$	≈0.26	Calc. detected	17,111 24,26,31
12	Mg($3s3p\ ^3P$)	$3d3p^2\ ^4P^e$	≈0.35	Calc. detected	17,111 24,26
18	Ar($3p^5 4s\ ^3P$)	$3p^5 4s4p\ ^4S^e$	>0	Calc.	17
20	Ca($4s4p\ ^3P$)	$4s4p^2\ ^4P^e$	≈0.55	Calc. detected	17 26,55
30	Zn($4s4p^3P$)	$4s4p^2\ ^4P^e$	>0	Calc. detected	17 26
38	Sr($5s5p^3P$)	$5s5p^2\ ^4P^e$		detected	26
48	Cd($5s5p^3P$)	$5s5p^2\ ^4P^e$		detected	26
56	Ba($6s6p^3P$)	$6s6p^2\ ^4P^e$		detected	26
80	Hg($6s6p^3P$)	$6s6p^2\ ^4P^e$		detected	26

7. Acknowledgments

As always, we are especially pleased to acknowledge the key role played by our many "negative ion" colleagues and students. Much of the work reported here has been supported by the National Science Foundation and the Deutsche Forschungsgemeinschaft. We both appreciate the expert assistance of Leslie Haas, Gwendy Lykke, and Lorraine Volsky in the preparation of this manuscript. The support and encouragement of the JILA Data Center in this work is certainly appreciated. H.H. gratefully acknowledges the hospitality granted by the Joint Institute for Laboratory Astrophysics. W.C.L. is pleased to acknowledge the Council on Research and Creative Work of the University of Colorado for a Faculty Fellowship.

8. References

[1]H. Hotop and W. C. Lineberger, J. Phys. Chem. Ref. Data **4**, 539 (1975).
[2]H. S. W. Massey, Endeavour **35**, 58 (1976).
[3]R. R. Corderman and W. C. Lineberger, Ann. Rev. Phys. Chem. **30**, 347 (1979).
[4]B. K. Janousek and J. I. Brauman, in *Gas Phase Ion Chemistry*, edited by M. T. Bowers (Academic, New York, 1979), Vol. 2, pp. 53–86.
[5]T. M. Miller, Adv. Electron. Electron Phys. **55**, 119 (1981).
[6]J. T. Moseley, in *Applied Atomic Collision Physics*, edited by H. S. W. Massey, E. W. McDaniel, and B. Bederson (Academic, New York, 1982), Vol. 5, p. 269; J. Durup and J. T. Moseley, Ann. Rev. Phys. Chem. **32**, 53 (1981).
[7]R. D. Mead, A. E. Stevens, and W. C. Lineberger, in *Gas Phase Ion Chemistry*, edited by M. T. Bowers (Academic, New York, 1984), Vol. 3, pp. 213–248.
[8]P. S. Drzaic, J. Marks, and J. I. Brauman, in *Gas Phase Ion Chemistry*, edited by M. T. Bowers (Academic, New York, 1984), Vol. 3, pp. 167–211.
[9]H. S. W. Massey, in *Negative Ions*, 3rd ed. (Cambridge University, London, 1976).
[10]E. H. Lieb, Phys. Rev. A **29**, 3018 (1984).
[11]J. S. Sims, S. A. Hagstrom, D. Munch, and C. F. Bunge, Phys. Rev. A **13**, 560 (1976).
[12]C. F. Bunge and A. V. Bunge, Int. J. Quantum Chem. Symp. **12**, 345 (1978).
[13]R. Jáuregui and C. F. Bunge, J. Chem. Phys. **71**, 4611 (1979).
[14]A. V. Bunge and C. F. Bunge, Phys. Rev. A **19**, 452 (1979).
[15]C. F. Bunge, Phys. Rev. A **22**, 1 (1980); C. F. Bunge, Phys. Rev. Lett. **44**, 1450 (1980).
[16]K. Raghavachari, J. Chem. Phys. **82**, 4142 (1985).
[17]C. F. Bunge, M. Galán, R. Jáuergui, and A. V. Bunge, Nucl. Instrum. Methods **202**, 299 (1982).
[18]C. A. Nicolaides, Y. Komninos, and D. R. Beck, Phys. Rev. A **24**, 1103 (1981); D. R. Beck, Phys. Rev. A **27**, 1187 (1983); Phys. Rev. A **30**, 3305 (1984).
[19]A. U. Hazi and K. Reed, Phys. Rev. A **24**, 2269 (1981).
[20]C. L. Pekeris, Phys. Rev. **112**, 1649 (1958); Phys. Rev. **126**, 1470 (1962).
[21]K. Aashamar, Nucl. Instrum. Methods **90**, 263 (1970).
[22]E. P. Wigner, Phys. Rev. **73**, 1002 (1948).
[23]J. T. Broad and W. P. Reinhardt, Phys. Rev. A **14**, 2159 (1976).
[24]K. Bethge, E. Heinicke, and H. Baumann, Phys. Lett. **23**, 542 (1966).
[25]E. Heinicke, K. Bethge, and H. Baumann, Nucl. Instrum. Methods **58**, 125 (1968).
[26]H. J. Kaiser, E. Heinicke, H. Baumann, and K. Bethge, Z. Phys. **243**, 46 (1971).
[27]H. V. Smith, Jr. and H. T. Richards, Nucl. Instrum. Methods **125**, 497 (1975).
[28]R. Middleton, Nucl. Instrum. Methods **144**, 373 (1977).
[29]G. Braun-Elwert, J. Huber, G. Korschinek, W. Kutschera, W. Goldstein, and R. L. Hershberger, Nucl. Instrum. Methods **146**, 121 (1977).
[30]Y. K. Bae, M. J. Coggiola, and J. R. Peterson, Phys. Rev. A **29**, 2888 (1984).
[31]Y. K. Bae and J. R. Peterson, Phys. Rev. A **30**, 2145 (1984).
[32]F. Sasaki and M. Yoshimine, Phys. Rev. A **9**, 26 (1974).
[33]L. A. Cole and J. P. Perdew, Phys. Rev. A **25**, 1265 (1982).
[34]R. J. Zollweg, J. Chem. Phys. Lett. **50**, 4251 (1969).
[35]B. M. Angelov, Chem. Phys. Lett. **43**, 368 (1976).
[36]S. G. Bratsch, Chem. Phys. Lett. **98**, 113 (1983).

[37]S. G. Bratsch and J. J. Lagowski, Chem. Phys. Lett. **107**, 136 (1984).
[38]W. C. Lineberger and B. W. Woodward, Phys. Rev. Lett. **25**, 424 (1970).
[39]H. Hotop, T. A. Patterson, and W. C. Lineberger, Phys. Rev. A **8**, 762 (1973).
[40]H. Hotop and W. C. Lineberger, J. Chem. Phys. **58**, 2379 (1973).
[41]T. A. Patterson, H. Hotop, A. Kasdan, D. W. Norcross, and W. C. Lineberger, Phys. Rev. Lett. **32**, 189 (1974).
[42]B. Brehm, M. A. Gusinow, and J. L. Hall, Phys. Rev. Lett. **19**, 737 (1967).
[43]M. W. Siegel, R. J. Celotta, J. L. Hall, J. Levine, and R. A. Bennett, Phys. Rev. A **6**, 607 (1972).
[44]R. J. Celotta, R. A. Bennett, J. L. Hall, M. W. Siegel, and L. Levine, Phys. Rev. A **6**, 631 (1972).
[45]H. Hotop, R. A. Bennett, and W. C. Lineberger, J. Chem. Phys. **58**, 2373 (1973).
[46]A. Kasdan and W. C. Lineberger, Phys. Rev. A **10**, 1658 (1974).
[47]W. H. Wing, G. A. Ruff, W. E. Lamb, Jr., and J. J. Spezeski, Phys. Rev. Lett. **36**, 1488 (1976).
[48]S. L. Kaufman, Opt. Commun. **17**, 309 (1976).
[49]B. A. Huber, T. M. Miller, P. C. Cosby, H. D. Zeman, R. L. Leon, J. T. Moseley, and J. R. Peterson, Rev. Sci. Instrum. **48**, 1306 (1977).
[50]A. Carrington, Proc. R. Soc. London Ser. A **367**, 433 (1979).
[51]U. Hefter, R. D. Mead, P. A. Schulz, and W. C. Lineberger, Phys. Rev. A **28**, 1429 (1983); R. D. Mead, U. Hefter, P. A. Schulz, and W. C. Lineberger, J. Chem. Phys. **82**, 1723 (1985).
[52]R. Morgenstern, A. Niehaus, and U. Thielmann, Abstracts of Papers, *9th International Conference on the Physics of Electronic and Atomic Collisions* (University of Washington, Seattle, 1975), p. 870; J. Phys. B **10**, 1039 (1977).
[53]P. Dahl, M. Rødbro, B. Fastrup, and M. E. Rudd, J. Phys. B **9**, 1567 (1976).
[54]D. Feldmann, R. Rackwitz, E. Heinicke, and H. J. Kaiser, Phys. Lett. A **45**, 404 (1973).
[55]E. Heinicke, H. J. Kaiser, R. Rackwitz, and D. Feldmann, Phys. Lett. A **50**, 265 (1974).
[56]H. J. Kaiser, E. Heinicke, R.Rackwitz, and D. Feldmann, Z. Phys. **270**, 259 (1974).
[57]D. Feldmann, Z. Phys. A **277**, 19 (1976).
[58]D. Feldmann, Chem. Phys. Lett. **47**, 338 (1977).
[59]D. Feldmann, R. Rackwitz, E. Heinicke, and H. J. Kaiser, Z. Naturforsch. A **32**, 302 (1977).
[60]D. Feldmann, R. Rackwitz, E. Heinicke, and H. J. Kaiser, Z. Phys. A **282**, 143 (1977).
[61]R. R. Corderman, P. C. Engelking, and W. C. Lineberger, Appl. Phys. Lett. **36**, 533 (1980).
[62]C. S. Feigerle, R. R. Corderman, S. V. Bobashev, and W. C. Lineberger, J. Chem. Phys. **74**, 1580 (1981).
[63]C. S. Feigerle, R. R. Corderman, and W. C. Lineberger, J. Chem. Phys. **74**, 1513 (1981).
[64]C. S. Feigerle, Z. Herman, and W. C. Lineberger, J. Electron Spectrosc. Relat. Phenom. **23**, 441 (1981).
[65]J. R. Peterson, M. J. Coggiola, and Y. K. Bae, Phys. Rev. Lett. **50**, 664 (1983).
[66]D. Feldmann, Phys. Lett. A **53**, 82 (1975).
[67]J. Slater, F. H. Read, S. E. Novick, and W. C. Lineberger, Phys. Rev. A **17**, 201 (1978).
[68]P. L. Jones, R. D. Mead, B. E. Kohler, S. D. Rosner, and W. C. Lineberger, J. Chem. Phys. **73**, 4419 (1980).
[69]P. Frey, F. Breyer, and H. Hotop, J. Phys. B **11**, L589 (1978).
[70]P. Frey, M. Lawen, F. Breyer, H. Klar, and H. Hotop, Z. Phys. A **304**, 155 (1982).
[71]R. A. Falk, D. Leep, and R. Geballe, Phys. Rev. A **22**, 1099 (1980).
[72]N. Rouze and R. Geballe, Phys. Rev. A **27**, 3071 (1983).
[73]W. A. M. Blumberg, R. M. Jopson, and D. J. Larson, Phys. Rev. Lett. **40**, 1320 (1978).
[74]S. A. Lee and J. L. Hall, Appl. Phys. Lett. **25**, 367 (1976).
[75]R. Balhorn, H. Kunzmann, and F. Lebowsky, Appl. Opt. **11**, 742 (1972).
[76]F. Breyer, P. Frey, and H. Hotop, Z. Phys. A **286**, 133 (1978).
[77]F. Breyer, P. Frey, and H. Hotop, Z. Phys. A **300**, 7 (1981).
[78]C. S. Feigerle, A. E. Stevens, D. Spence, S. M. Burnett, and W. C. Lineberger, Rev. Sci. Instrum. (in preparation).
[79]J. E. Pollard, D. J. Trevor, Y. T. Lee, and D. A. Shirley, Rev. Sci. Instrum. **52**, 1837 (1981); P. J. Hicks, S. David, B. Wallbank, and J. Comer, J. Phys. E **13**, 713 (1980); L. Asbrink and J. W. Rabalais, Chem. Phys. Lett. **12**, 182 (1971).
[80]P. A. M. Gram, J. C. Pratt, M. A. Yates-Williams, H. C. Bryant, J. Donahue, H. Sharifian, and H. Tootoonchi, Phys. Rev. Lett. **40**, 107 (1978)
[81]M. E. Hamm, R. W. Hamm, J. Donahue, P. A. M. Gram, J. C. Pratt, M. A. Yates, R. D. Bolton, D. A. Clark, H. C. Bryant, C. A. Frost, and W. W. Smith, Phys. Rev. Lett. **43**, 1715 (1979).
[82]J. B. Donahue, P. A. M. Gram, M. V. Hynes, R. W. Hamm, C. A. Frost, H. C. Bryant, K. B. Butterfield, D. A. Clark, and W. W. Smith, Phys. Rev. Lett. **48**, 1538 (1982).
[83]D. M. Neumark, K. R. Lykke, T. Andersen, and W. C. Lineberger, Phys. Rev. A (in press).
[84]R. D. Mead, K. R. Lykke, and W. C. Lineberger (unpublished).
[85]J. R. Peterson, Y. K. Bae, and D. L. Huestis, Post-deadline paper, ICAP, Seattle, 1984.
[86]Y. K. Bae and J. R. Peterson, Phys. Rev. A (in press).
[87]D. J. Larson and R. Stoneman, Phys. Rev. A **31**, 2210 (1985).
[88]J. E. M. Goldsmith and J. E. Lawler, Contemp. Phys. **22**, 235 (1981).
[89]C. R. Webster and C. T. Rettner, Laser Focus, February (1983).
[90]C. R. Webster, I. S. McDermid, and C. T. Rettner, J. Chem. Phys. **78**, 646 (1983).
[91]I. S. McDermid and C. R. Webster, J. Phys. (Paris) **44**, C7-461 (1983).
[92]R. Klein, R. P. McGinnis, and S. R. Leone, Chem. Phys. Lett. **100**, 475 (1983).
[93]C. R. Webster (private communication).
[94]B. Steiner, Phys. Rev. **173**, 136 (1968).
[95]A. Kasdan, E. Herbst, and W. C. Lineberger, J. Chem. Phys. **62**, 541 (1975).
[96]P. C. Engelking and W. C. Lineberger, Phys. Rev. A **19**, 149 (1979).
[97]R. R. Corderman, P. C. Engelking, and W. C. Lineberger, J. Chem. Phys. **70**, 4474 (1979).
[98]A. R. P. Rau and U. Fano, Phys. Rev. A **4**, 1751 (1971).
[99]A. R. P. Rau, in *Electron and Photon Interactions with Atoms*, edited by H. Kleinpoppen and M. R. C. McDowell (Plenum, New York, 1976), p. 141.
[100]P. A. Cox, Struct. Bonding (Berlin) **24**, 59 (1975).
[101]J. Schirmer, L. S. Cederbaum, and J. Kiessling, Phys. Rev. A. **22**, 2696 (1980).
[102]R. M. Stelman, W. B. Clodius, S. Grot, and S. D. Woo, Phys. Rev. A **31**, 297(1985).
[103]D. G. Leopold, K. K. Murray, and W. C. Lineberger, J. Chem. Phys. **81**, 1048 (1984).
[104]H. B. Ellis, Jr. and G. B. Ellison, J. Chem. Phys. **78**, 6541 (1983).
[105]K. Bowen (private communication).
[106]C. S. Feigerle, Ph.D. thesis (University of Colorado, 1983) (unpublished).
[107]H. Baumann, E. Heinicke, H. J. Kaiser, and K. Bethge, Nucl. Instrum. Methods **95**, 389 (1971).
[108]D. Spence, W. A. Chupka, and C. M. Stevens, Phys. Rev. A **26**, 654 (1982).
[109]P. Rohwer, H. Baumann, K. Bethge, and W. Schütze, "Jahresbericht 1982," Institut für Kernphysik, Universität Frankfurt, Frankfurt, 1982, pp. 105–6.
[110]E. R. Cohen and B. N. Taylor, J. Phys. Chem. Ref. Data **2**, 663 (1973); B. N. Taylor, Rev. Mod. Phys. **56**, 531 (1984).
[111]A. W. Weiss, Phys. Rev. **166**, 70 (1968).
[112]K. D. Jordan and J. Simons, J. Chem. Phys. **67**, 4027 (1977).
[113]J. Mazeau, F. Gresteau, R. I. Hall, and A. Huetz, J. Phys. B **11**, L557 (1978).
[114]H.-P. Popp, Z. Naturforsch. A **22**, 254 (1967).
[115]R. Milstein and R. S. Berry, J. Chem. Phys. **55**, 4146 (1971).
[116]P. A. Schulz, R. D. Mead, and W. C. Lineberger, Phys. Rev. A (in preparation).
[117]J. Slater and W. C. Lineberger, Phys. Rev. A **15**, 2277 (1977).
[118]G. Mück and H.-P. Popp, Z. Naturforsch. A **23**, 1213 (1968).
[119]H. Frank, M. Neiger, and H.-P. Popp, Z. Naturforsch. A **25**, 1617 (1970).
[120]R. S. Berry and C. W. Reimann, J. Chem. Phys. **38**, 1540 (1963).
[121]M. D. Scheer, J. Res. Natl. Bur. Stand. Sect. A **74**, 37 (1970).
[122]M. Hendewerk, Honors thesis (University of Colorado, 1981) (unpublished). Quoted in Ref. 7.
[123]P. D. Burrow, J. A. Michejda, and J. Comer, J. Phys. B **9**, 3225 (1976).
[124]K. Jost and B. Ohnemus, Phys. Rev. A **19**, 641 (1979); A. R. Johnson and P. D. Burrow, J. Phys. B. **15**, L745 (1982).
[125]D. L. Mader and R. Novick, in *Atomic Physics 3* (Plenum, New York, 1973), p. 169.
[126]C. J. Edge, N. B. Mansour, and D. J. Larson, Bull. Am. Phys. Soc. (in press).